Small-molecule screen identifies inhibitors of the neuronal K-Cl cotransporter KCC2

Eric Delpire[a,1], Emily Days[b], L. Michelle Lewis[b], Dehui Mi[b], Kwangho Kim[c], Craig W. Lindsley[c,d], and C. David Weaver[b,d]

[a]Department of Anesthesiology, [d]Department of Pharmacology, [c]Vanderbilt Specialized Chemistry Center, and [b]Vanderbilt Screening Center for GPCRs, Ion Channels, and Transporters, Vanderbilt University Medical Center, Nashville, TN 37232

Edited by Lily Y. Jan, University of California School of Medicine, San Francisco, CA, and approved February 4, 2009 (received for review December 16, 2008)

KCC2, a neuronal-specific K-Cl cotransporter, plays a major role in maintaining intracellular Cl^- concentration in neurons below its electrochemical equilibrium potential, thus favoring robust GABA hyperpolarizing or inhibitory responses. The pharmacology of the K-Cl cotransporter is dominated by loop diuretics such as furosemide and bumetanide, molecules used in clinical medicine because they inhibit the loop of Henle Na-K-2Cl cotransporter with much higher affinity. To identify molecules that affect KCC2 activity, we developed a fluorescence-based assay suitable for high-throughput screening (HTS) and used the assay to screen a library of 234,000 small molecules. We identified a large number of molecules that either decrease or increase the activity of the cotransporter. Here, we report the characterization of a small number of inhibitors, some of which inhibit KCC2 activity in the submicomolar range without substantially affecting NKCC1 activity. Using medicinal chemistry, we synthesized a number of variants, tested their effect on KCC2 function, and provide an analysis of structure/activity relationships. We also used one of the compounds to demonstrate competitive inhibition in regard to external [K^+] versus noncompetitive inhibition in respect to external [Cl^-].

fluorescence | high-througput screening | Na-K-2Cl cotransporter | thallium

Cation–chloride cotransporters have received much attention in the past decade for the role they play in the nervous system. In particular KCC2, a neuronal-specific K-Cl cotransporter, has been shown to modulate inhibitory neurotransmission both in the brain and in the spinal cord. By reducing the intracellular Cl^- concentration below its thermodynamic equilibrium potential in central neurons, KCC2 strengthens synaptic inhibition. Several studies have shown that loss of KCC2 function in central neurons results in the development of CNS hyperexcitability (1–3). Moreover, a paper from Coull and coworkers also showed that disinhibition in the dorsal horn of the spinal cord triggered by peripheral nerve injury was mediated by a significant decrease in KCC2 expression (4). Local blockade or knockdown of spinal KCC2 in intact rats markedly reduced the nocicepetive threshold. By linking change in KCC2 function to disruption of Cl^- homeostasis in lamina I neurons, the study clearly linked the loss of KCC2 function to a loss of inhibition in this region of the spinal cord and to an increase in chronic pain. The relationship between KCC2 and nerve or spinal cord injury has been confirmed in subsequent studies that have shown that inflammatory response due to intraplantar injection of formalin (5, 6) or hind paw injection of complete Freund's adjuvant (7), or to loose ligation of the sciatic nerve (8), or contusive spinal cord injury at T9 (9), all led to a down-regulation of cotransporter expression. Altogether, these studies also point to a role of KCC2 in neuropathic pain.

The pharmacology of the cation–chloride cotransporters is dominated by 2 classes of drugs: the thiazide and loop diuretics. Whereas thiazide diuretics target the apical Na-Cl cotransporter, located in the distal convoluted tubule, resulting in decreased salt reabsorption, loop diuretics (furosemide or LASIX and bumetanide or BUMEX), as their names imply, inhibit the apical Na-K-2Cl cotransporter, NKCC2, located in the thick ascending loop of Henle, thereby diminishing kidney salt reabsorption. They also inhibit NKCC1 in the micromolar range in isolated cells, but have little effect on NKCC1 in situ due to their binding to albumin in the circulation and consequently their poor access to peripheral tissues. High doses of diuretics have, however, ototoxic effects due to inhibition of NKCC1 in the inner ear (10–12). Furosemide and bumetanide also inhibit K-Cl cotransporter, including KCC2 but at much higher concentrations (100 μM–1 mM) (13–15). There are 2 compounds that inhibit K-Cl cotransport in the micomolar range: DIDS and DIOA, but their effect is species-specific (16, 17) and lacking in specificity with regard to other ion transporters and channels (for reviews, see refs. 18 and 19).

To identify molecules that affect the activity of KCC2, we developed a fluorescence-based method appropriate for high-throughput screening (HTS). Indeed, all traditional methods used to assess cation–chloride cotransporter activity are not adequate for HTS. The method makes use of a fluorescent dye sensitive to thallium, a cation that is transported by cation–chloride cotransporter. Thallium, in combination with dye, was previously used to assay uptakes of K^+ through K^+ channels (20). Using this method, we screened a library of 234,000 compounds with KCC2 as a target and identified a number of compounds that affect the activity of the cotransporter.

Results

To test thousands of compounds on the activity of KCC2, we needed to develop a method that was suitable for HTS. Although Cl^--sensitive dyes have been used to screen for inhibitors of CFTR and Ca^{2+}-activated Cl^- channels (21, 22), we wanted to test whether dyes that are sensitive to Tl^+ (thallium) a cation that permeates K^+ channels, would be suitable for HTS of cation–chloride cotransporters. To demonstrate that KCC2 transports thallium ($^{204}Tl^+$) at the K^+ site, we performed an experiment in which ^{86}Rb uptake was measured in KCC2-overexpressing HEK293 cells [see supporting information (SI) Fig. S1] incubated in solutions containing 2 mM $K_2(SO_4)$ or 2 mM $Tl_2(SO_4)$. As indicated in Fig. 1*A*, furosemide-sensitive ^{86}Rb uptake occurred in the presence of thallium, although somewhat reduced when compared with the K^+-containing solution. After loading KCC2-overexpressing or native HEK293 cells with a thallium fluorescent dye (BTC or fluozin-2), we measured the increase in

Author contributions: E. Delpire, C.W.L., and C.D.W. designed research; E. Delpire, E. Days, L.M.L., D.M., K.K., and C.D.W. performed research; E. Delpire, K.K., C.W.L., and C.D.W. contributed new reagents/analytic tools; E. Delpire, E. Days, L.M.L., C.W.L., and C.D.W. analyzed data; and E. Delpire, C.W.L., and C.D.W. wrote the paper.

The authors declare no conflict of interest.

This article is a PNAS Direct Submission.

Freely available online through the PNAS open access option.

[1]To whom correspondence should be addressed at: Department of Anesthesiology, Vanderbilt University Medical Center, T-4202 Medical Center North, 1161 21st Avenue South, Nashville, TN 37232. E-mail: eric.delpire@vanderbilt.edu.

This article contains supporting information online at www.pnas.org/cgi/content/full/0812756106/DCSupplemental.

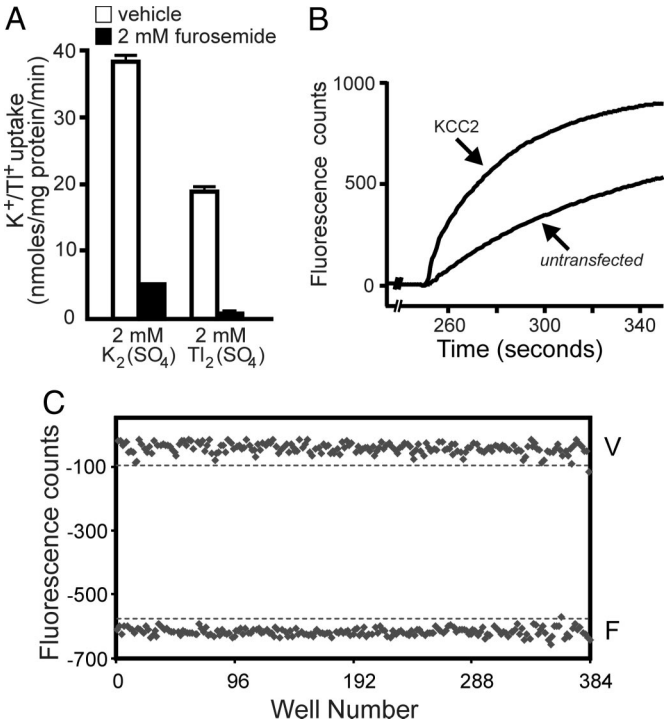

Fig. 1. KCC2-mediated thallim flux measurements. (*A*) Unidirectional ^{86}Rb uptake measured in KCC2-overexpressing HEK293 cells. Flux was performed in hypotonic solutions containing 4 mM K^+ or 4 mM Tl^+ in the presence and absence of 2 mM furosemide. Note the significant furosemide-sensitive Tl^+ uptake. (*B*) BTC fluorescence increase upon addition of thallium to KCC2-transfected and untransfected HEK293 cells. The fluorescence was recorded over a 6-min period. (*C*) Well-to-well reproducibility of the fluorescence method as demonstrated by fluorescence measurements performed in 384-well plates. Fluorescence data points on the upper trace represent 384 wells containing KCC2-overexpressing cells incubated in regular saline, whereas fluorescence data points on the lower trace represents similar conditions but with 2 mM furosemide. Note the significant separation between the 2 populations. The experiment was performed several times with identical results.

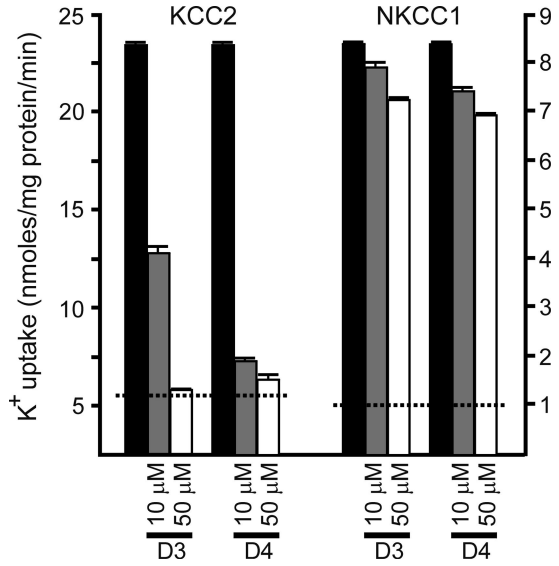

Fig. 2. Specific effect of compounds D3 and D4 on KCC2 versus NKCC1 function. Compounds were tested at doses of 10 and 50 μM on both KCC2-mediated and NKCC1-mediated (^{86}Rb) K^+-uptake. Dashed lines represent the basal flux, i.e., flux measured in the presence of 2 mM bumetanide. Bars represent means ± SEM (n = 3 dishes). The experiment was repeated once with similar results.

fluorescence elicited by the addition of thallium to the external solution. The increase was significantly higher in KCC2-overexpressing HEK293 cells, compared with native cells (Fig. 1*B*). The experiment was then repeated by using 2 384-well plates containing KCC2-overexpressing cells; in each plate, every other well was treated with vehicle control conditions, the others in the presence of 2 mM furosemide. As seen in Fig. 1*C*, the data derived from the initial slope of the thallium-evoked increase in fluorescence are very consistent from well to well, and the separation between the control and furosemide signals is very large. The Z′ value, defined as $1-(3SD_1 + 3SD_2)/\langle Ave_1 - Ave_2\rangle$, was measured at 0.78.

The screen was conducted in multiple 384-well plates containing HEK293 cells overexpressing KCC2. For each plate, 4 columns were dedicated to controls: 2 columns (32 wells) using standard HBSS conditions with ouabain and 2 columns using HBSS plus 2 mM bumetanide. These wells allowed for internal quality assessment. Each of the remaining 320 wells was dedicated to one compound tested at a concentration of nominally 10 μM. Using 733 plates, we screened 234,560 compounds with an average Z′ value of 0.686 ± 0.090, indicating both high fidelity and good separation between the 2 control signals (with and without bumetanide). Compounds that decreased or stimulated fluorescence signals >3 standard deviations from the test compound population measured on a per-plate basis were counted as primary hits. The screen yielded 4,933 hits (2%), with 1,880 compounds reducing and 2,954 compounds increasing the fluorescence signal, respectively.

After elimination of duplicates, a secondary screen was performed with 3,695 compounds. Each compound was tested in duplicate at a concentration of 10 μM by using both KCC2-overexpressing cells and naïve HEK293 cells. With each cell line, the secondary screen was performed in the presence and absence of ouabain. Approximately 60% of the compounds (2,224) verified. We identified 465 compounds that were positive in KCC2-overexpressing cells, but not in naïve HEK293 cells, irrespective of the presence or absence of ouabain. Each of the 465 compounds was then tested at various concentrations (ranging from 0.5 nM to 30 μM) in triplicate, and ≈76% of them displayed a typical dose dependence.

Based on their potency and structure, we selected 26 compounds that inhibited thallium-induced fluorescence increase and tested them on KCC2 and NKCC1 functions by using ^{86}Rb uptakes in HEK293 cells. For KCC2, we used *N*-ethylmaleimide pretreatment in KCC2-overexpressing HEK293 cells. The alkylating agent not only stimulates K-Cl cotransport, but abrogates the function of the native Na-K-2Cl cotransporter (Fig. S2). For NKCC1, we used a hyperosmotic solution to stimulate the transporter in naïve HEK293 cells (Fig. S2). Table S1 lists the efficacy of each of the 26 compounds on KCC2 and NKCC1 function. As seen in the table, some compounds like D4 inhibit KCC2 with a measured IC_{50} in the submicromolar range while minimally affecting NKCC1. In contrast, other compounds like D8 acted equally well on KCC2 and NKCC1.

To compare further the specificity of D3 and D4 on KCC2 over NKCC1, we plotted the data of K^+ uptakes (in nmol/mg of protein/min) at compounds concentrations of 10 μM and 50 μM. As seen in Fig. 2, both D3 and D4 inhibited significantly KCC2-mediated K^+ uptake at 10 μM, whereas they only showed a small effect on NKCC1-mediated K^+ uptake. Furthermore, this small effect was not significantly increased by increasing the dose to 50 μM, indicating a lack of dose–response. Fig. 3 presents full dose–response curves for compounds D4 and bumetanide. It shows 3 orders of magnitude difference in the IC_{50}. A similar low affinity was found for furosemide (see IC_{50} in Table S1).

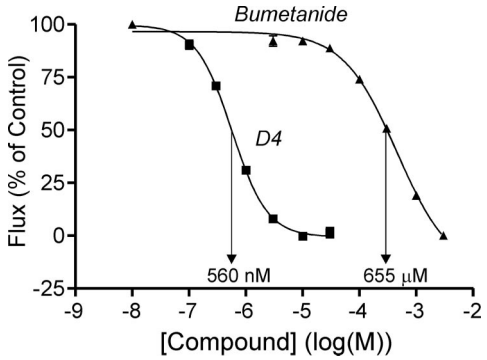

Fig. 3. Dose–response curve of compounds D4 and bumetanide on KCC2 function. K^+ uptakes were measured in triplicate in KCC2-overexpressing cells at different concentrations of inhibitors ranging from 100 nM to 30 μM (D4) and 30 μM to 3 mM (bumetanide). Flux was expressed as a percentage of control (flux without inhibitor). Arrows point to individual IC_{50} values.

To gain information on structure–activity relationship (SAR), we synthesized a number of molecules around the structure of D4, *N*-(4-methylthiazol-2-yl)-2-(6-phenylpyridazin-3-ylthio)acetamide. We designed a small 13-member library wherein the Western 6-phenylpyridazine moiety was held constant, while varying the eastern heterocycle, i.e., the 4-methyl thiazole, with differentially functionalized thiazoles and pyridines. The synthetic route to the analogs **6a**-**6m** as well as the resynthesis of D4 is shown in Fig. S3. Commercial 3-chloro-6-phenylpyridazine **1** is treated with thiourea under microwave irradiation for 15 min to afford the corresponding 6-phenylpyridazine-3-thiol **2** in 83% isolated yield. Concurrently, 13 heterocyclic amines **3** were exposed to 2-chloroacetyl chloride **4** to afford 13 derivative **5** in 85–95% yield. Finally, the 13 derivative **5** were reacted with 6-phenylpyridazine-3-thiol **2** to deliver D4 congeners **6a**-**6m** in 38–56% isolated yields. The parent D4 was also resynthesized in 48% yield following this route by reacting **2** and **7**, 2-chloro-*N*-(4methylthiazol-2-yl)acetamide. SAR for this series was rather flat, with functionalized pyridines, **6a**-**6f**, affording <32% inhibition of KCC2 at 1 μM (Fig. 4). If the 4-methyl group was removed from D4, as in **6g**, inhibition was greatly diminished. Various alkly replacements in the 4 position of the thiazole moiety were tolerated, **6i**-**6k**, providing good inhibition (56–62%) at 1 μM. D4 (**6l**) confirmed upon resynthesis (IC_{50} = 558 nM and selective versus NKCC1) as did an *N*-Me amide congener **6m** of D4 (IC_{50} = 537 nM and selective versus NKCC1).

Compounds D4 (**6l**) and **6m** were also tested against 68 GPCRs, ion channels and transporters at MDS Pharma. This ancillary pharmacology screen showed significant response (>50% at 10 μM) for 6l with 4 targets (Adenosine A1 and A3 receptors, L- type Ca^{2+} channel, and K^+ channel hERG), but no response for **6m**, indicating increased specificity by substituting the NH group of D4 (**6l**) to a tertiary *N*-Me amide group (see Table S2).

Finally, important information on the modality of inhibitor binding can be gained by performing transport kinetic experiments. In a first experiment, we tested the effect of D4 on KCC2 function, measured at different external K^+ concentrations. The data, presented as 1/Flux versus 1/[K] (Lineweaver–Burke plot Fig. 5*A1*) are consistent with competitive inhibition. However, because the intercept was very close to the *x* axis, we replotted the data as [K]/Flux versus [inhibitor] (Hanes-Woolf plot, Fig. 5*A2*) and confirmed through all parallel lines (unique slope) the nature of the competitive inhibition. These data clearly indicate that the inhibitor binds to the transporter before K^+, i.e., once K^+ is bound to the cotransporter, the inhibitor is unable to bind. In a second experiment, we tested the external Cl^- concentration on D4 binding and KCC2 function. Interestingly, the double-reciprocal plot was now typical of a noncompetitive inhibition, because all lines intercepted on the *y* axis (Fig. 5*B*). The affinity for Cl^- was extracted from the intercept and calculated to be 59 mM. Altogether, our data demonstrate that the inhibitor binds noncompetitively with respect to Cl^- ions but competitively with respect to K^+ ions. The only model compatible with these data allows (*i*) the random binding of K^+ and Cl^- ions to the unoccupied transporter, and (*ii*) the binding of the inhibitor only to K^+-unoccupied transporters (Fig. 5*C*). Derivations of the rapid equilibrium equations for this model are provided in *SI Text*. Ordered ion-binding models (K^+ binding first followed by Cl^- or vice versa) are rejected on the basis that competitive

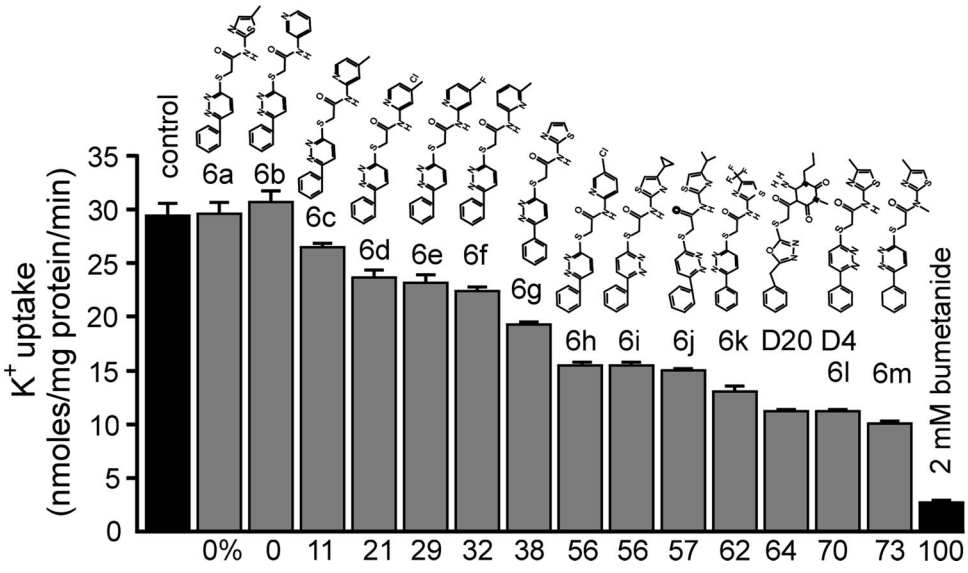

Fig. 4. Chemical modifications around D4 scaffold and effect on KCC2-mediated K^+ uptake. Structure variants were synthesized, confirmed by mass spectrometry, and tested at 1 μM on KCC2 function. Filled bars represent of K^+ uptake in KCC2-overexpressing cells under control and 2 mM bumetanide conditions. Each gray bar represents the uptake in the presence of 1 μM inhibitor. Numbers under the bars indicate the percentage inhibition, calculated based on the control and bumetanide data. All bars represent mean ± SEM (n = 3 dishes).

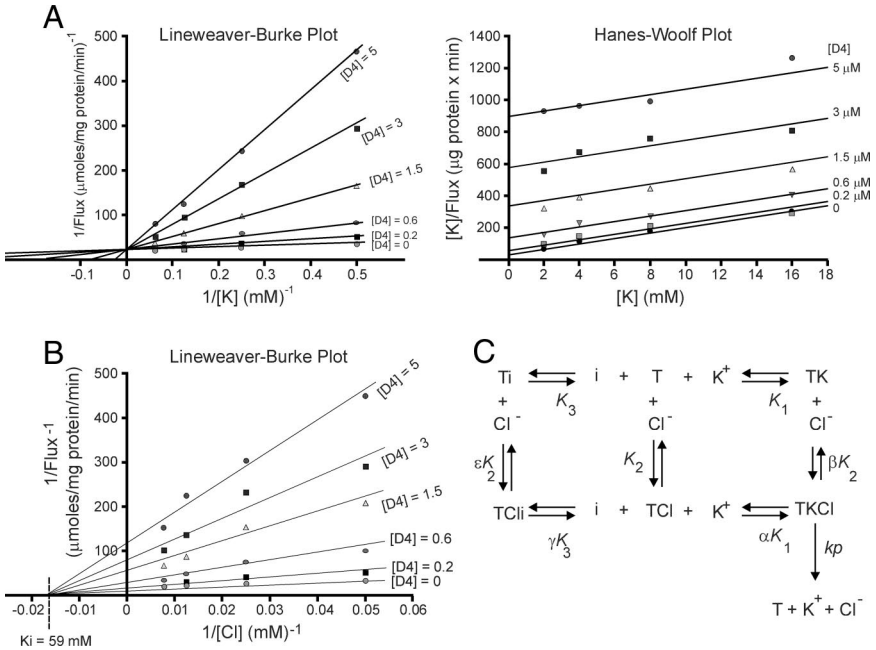

Fig. 5. Kinetic analysis of D4 inhibition. (*A*) D4 inhibition as a function of external [K^+]. Data are plotted as Lineweaver–Burke (*A1*) and Hanes–Woolf (*A2*) plots. Note the single intercept of the lines on the *y* axis in the Lineweaver–Burke plot and the single slope of the lines in the Hanes–Woolf Plot. (*B*) D4 inhibition as a function of external [Cl^-], with data plotted as Lineweaver–Burke plot. Note the single intercept of the lines on the *x* axis yielding a K_i for Cl^- of 59 mM. All data were fitted with linear regression using GraphPad Prizm, version 3, software. (*C*) Kinetic model of KCC2 inhibition by inhibitor D4 based on the data from *A* and *B*. The velocity equations, derived according to ref. 41, are available as *SI Text*.

inhibition was demonstrated with K^+ (K^+-first model) and that the intercept of the lines in the Lineweaver–Burke plot (1/Flux versus 1/[Cl]) is unique on the *x* axis (Cl^--first model).

Discussion

Since its molecular identification in 1996 (23), the physiology of KCC2, a neuronal K-Cl cotransporter, has received increasing attention. In the absence of potent and specific pharmacological agents, the function of the cotransporter has been resting on studies using high doses of furosemide (24–26) and studies relying on genetic models such as KCC2 knockout and hypomorhic mice (1, 2, 27, 28), *Drosophila* KCC knockout (29), and transgenic zebrafish (30).

Furosemide or frusemide came in the early 1960s as a new and powerful diuretic developed by Farbwerke Hoechst in Germany and marketed under the trade name of Lasix (31). Together with bumetanide (32), these 2 drugs have been widely used as diuretics, targeting the thick ascending-limb loop of Henle's Na-K-2Cl cotransporter. Both bumetanide and furosemide bind to NKCC with 0.5–5 μM affinities. The discovery in the early 1980s of a Cl^--sensitive K^+ flux pathway, K-Cl cotransport, came with information regarding its sensitivity to much higher doses of loop diuretics (13, 33, 34). Since then, the diuretics have been widely used as inhibitor of K-Cl cotransporter, despite the discovery of other compounds that can inhibit K-Cl cotransporter with higher potency. These drugs, such as DIDS (16) or DIOA (35) affect K-Cl cotransport in species-specific manner, have multiple other targets, and have been reported to affect cell viability.

Animal models in which expression of KCC2 has been genetically manipulated have provided significant information on the role of KCC2 in maintaining a lower-than-equilibrium intracellular Cl^- concentration, facilitating hyperpolarizing GABA responses (for review, see ref. 36). Indeed, electroneutral and tightly coupled K-Cl cotransport is able to drive Cl^- ions against its own electrochemical gradient by using energy from the large gradient or distribution of potassium across the plasma membrane, which is generated by the Na^+/K^+-ATPase. The switch of GABA from depolarization to hyperpolarization and the strengthening of GABA hyperpolarizing responses arise concomitantly with a significant increase in KCC2 expression during postnatal development (reviewed in ref. 37). KCC2 has also been recently implicated in the neuropathic pain pathway, because its inhibition or down-regulation led to a marked reduction in nociceptive threshold (4).

A significant informative finding of this study is the development of an assay to assess cation–chloride cotransporter function. Indeed, our study make use of fluorescent dyes that are typically sensitive to divalent cations, such as Ca^{2+} for BTC and Zn^{2+} for fluozin-2, and the use of a monovalent cation Tl^+ (thallium), which interacts with these dyes. Note that Ca^{2+} quenches whereas Tl^+ increases BTC fluorescence. These thallium-sensitive dyes were screened and identified by one of us and used to assess, through fluorescence, the movement of thallium through K^+ channels (20). Although we demonstrated that Tl^+ is transported by KCC2 (Fig. 1*A*) and NKCC1 on the K^+ site, it is clear that unlike Rb^+, Tl^+ is not transported equally to K^+. This could be due to a lower affinity of the cotransporters for Tl^+ or to a reduced ability of the cotransporter to translocate Tl^+ and Cl^- ions across the plasma membrane. This will need to be resolved in other studies. Despite this reduced flux, we showed that the methodology is robust and suitable for HTS.

A second critical informative finding of this study is the identification of pharmacological inhibitors of KCC2. Our primary and secondary screens identified a rather large number of compounds that inhibit and activate KCC2. In this study, we focused on a series of inhibitory compounds that passed several filters, including specificity to the KCC2-overexpressing cell line versus naïve HEK293 cells as well as the production of typical dose–response curves. Although we have identified several potential scaffolds (Table S1), we focused our attention on compound D4 (Pubchem SID# 24814385) because its submi-

cromolar potency (Fig. 3), its specificity to KCC2 versus NKCC1 (Fig. 2), and its similarity to 2 other compounds identified in the screen (D12 and D20). The synthesis of structural analogs with various degrees of activity is also extremely useful for future optimization of drug properties. Preliminary SAR work reveals that the thiazole moiety of D4 is essential for activity and that several alkyl substituents in the 4 position of the thiazole are tolerated (56–70% inhibition at 1 μM). Moreover, both D4 (**6l**) and an *N*-Me amide congener, **6m**, are equipotent (EC_{50}s of 558 nM and 537 nM, respectively) and possess unprecedented selectivity versus the closely related NKCC1. Based on the 3 log-order increase in KCC2 inhibitory activity versus bumetanide and the selectivity versus NKCC1, D4 (**6l**) was declared an MLPCN probe compound for KCC2 and ascribed the PubChem identifier SID 56405457.

Finally, another significant finding of this study is the characterization of inhibitor binding with respect to both external K^+ and Cl^- ions. To determine the nature of D4 binding to KCC2, we used the enzyme kinetic approach assuming rapid equilibrium (see ref. 38) and *SI Text*). We measured D4 inhibition at different external K^+ concentrations as well as D4 inhibition at various Cl^- concentrations. We demonstrated that D4 was binding to KCC2 competitively with K^+ ions, but noncompetitively with Cl^- ions. Interestingly, competitive inhibition with K^+ ions and noncompetitive inhibition with Cl^- ions was suggested by data obtained with furosemide in red blood cells (13), indicating a similar mechanism of action. Whether the compounds identified in this study bind to the same site on KCC2 will need to be addressed in future studies. All possible models of D4, K^+, and Cl^- binding to KCC2 were drawn and velocities equations derived. Our data are only well-suited to the model presented in Fig. 5*C*, in which K^+ and Cl^- ions bind randomly to the cotransporter, and in which D4 does not bind to a K^+-attached carrier. Furthermore, our results also indicate that the binding of Cl^- to the transporter does not affect the binding of K^+ (because the unique intercept on the *x* axis in Fig. 5*B* requires the factor α to be 1); as the binding of Cl^- to the transporter also does not affect the binding of D4 (for a similar reason and $\gamma = 1$). These data were somewhat surprising, as we had demonstrated in the past ordered ion binding for K^+ and Cl^- outside the sheep red blood cell K-Cl cotransporter (39, 40). This discrepancy might indicate isoform-specific differences, difference in the membrane environments between the 2 systems, or different kinetic properties depending on the mode of KCC activation.

In summary, we report the development and validation of an efficient screen for identification of inhibitors of cation–chloride cotransporters. We identified a number of molecules that inhibit KCC2 function. Additional studies will be required to further define the specificity of these molecules, including specificity among the 4 K-Cl cotransporters. As this manuscript goes to press, we determined that D4 also inhibits KCC3 in the micromolar range, indicating that this compound does not distinguish between these 2 K-Cl cotransporters. Whether specificity can be obtained by modifying the chemical structure will be tested in future work Additional studies will also be required to test efficacy of these compounds on the cotransporter in native tissue. The development of these tools should have an impact on studies of KCC2 in preventing brain hyperexcitability and in gating pain information in the dorsal horn of the spinal cord.

Materials and Methods

HEK293 Cell Culture. Wild-type or KCC2-expressing HEK293 cells were grown up to 80–90% confluence in 10-cm dishes containing DMEM/Ham's F-12 (1:l) (Invitrogen) supplemented with 10% FBS (JRH Biosciences), 50 units/mL penicillin, and 50 pg/mL streptomycin (Invitrogen). KCC2-expressing clones were under puromycin selection (2 μg/mL; Sigma). Cultures were maintained at 37 °C in the presence of 5% CO_2. Cells were passaged every 3–4 days, using a ratio of 1:10, for a maximum of 16 passages. For fluorescence measurements, the cells were plated in T175 flasks 4 days before the assay.

Tl-Induced Fluozin-2 Fluorescence Increase. The day before the experiment, cells were plated in 384-well, black-walled, clear-bottom, polyD-lysine coated plates (Greiner Bio-One) at a concentration of 20,000 cells per well by using a Multidrop Combi (Thermo Fisher). The medium was removed by using an ELx405CW cell washer (BioTek) and replaced with 20 μL of HBSS plus 20 mM Hepes (pH 7.3) and 20 μL of HBSS plus 20 mM Hepes (pH 7.3) containing 2 μM fluozin-2 dye (Invitrogen) plus 0.2% (wt/vol) Pluronic F-127 (Invitrogen) by using a Multidrop Combi. Cells were incubated with the dye at room temperature for 48 min. The wells were then washed 3 times with HBSS plus 20 mM Hepes (addition of 80 μL and aspiration to leave $\approx$20 μL) by using the ELx405CW. After the washes, the cell plate was inserted into a Hamamatsu FDSS 6000 and precompound-addition fluorescence counts were obtained (5 frames at 1 Hz, excitation 470 $\pm$ 20 nm, emission 540 $\pm$ 30 nm), In parallel, 70 nL per well of compounds from 10 mM (nominal) stocks in DMSO supplied as the Molecular Libraries Small Molecule Repository collection by BioFocus DPI were transferred to 384-well polypropylene plates (Greiner) by using an Echo 555 (Labcyte) and diluted with 35 μL per well HBSS plus 20 mM Hepes (pH 7.3) and 200 μM ouabain using a Multidrop Combi. Twenty microliters per well of the diluted compounds were then added to the dye-loaded cell plates by using a Velocity11 Bravo and incubated for 8 min. Next, the compound-treated cell plates were loaded back onto the FDSS 6000. After 10 s, 10 μL per well of 5$\times$ thallium stimulus buffer [125 mM sodium bicarbonate, 12 mM thallium sulfate, 1 mM magnesium sulfate, 1.8 mM calcium sulfate, 5 mM glucose, 10 mM Hepes (pH 7.3)] was added. All steps of the screening protocol after compound plating were accomplished by using an automated screening system. Plates were moved by using a Thermo Fisher F3 robotic arm and all instruments and scheduling were under the control of Thermo Fisher Polara scheduling software version 2.3. After normalizing each well's fluorescence trace by dividing each data point after compound addition by the initial fluorescence values obtained on the FDSS precompound addition, activity was measured by obtaining the initial values of the slope of Tl^+-stimulated fluorescence increase by using linear regression. Hits were selected as compounds that caused a decrease in the slope of $\geq$3 standard deviations from the general population of test wells. Hits were reordered from BioFocus DPI and retested in duplicate. Retest-positive compounds were further evaluated by testing them at varying concentrations on both the KCC2-expressing cell line and the parental untransfected HEK cells. Compounds displaying selective, concentration-dependent activity were selected for further evaluation.

^{86}Rb Assays in HEK293 Cells. For rubidium uptake assays, cells were briefly trypsinized from 10-cm dishes and plated for 2 h on 35-mm dishes coated with polyL-Lysine (0.1 mg/mL; Sigma). Cells were washed once and preincubated for 15 min with 1 mL of hyposmotic saline solution containing 120 mM NaCl, 5 mM KCl, 2 mM $CaCl_2$, 0.8 mM $MgSO_4$, 5 mM Hepes, 5 mM glucose, 100 μM ouabain, 500 μM *N*-ethylmaleimide (pH 7.4) with HCl (260–270 mOsm). After the preincubation period, the medium was aspirated and replaced with 1 mL of similar solution without NEM, but containing 1 μCi/mL ^{86}Rb (PerkinElmer). After 15-min uptake, the solution was aspirated, and the cells were washed 3 times with ice-cold solution. Time-course experiments have shown that the flux is linear over a 30-min period. The cells were then lysed for 1 h with 500 μL of 0.25 M NaOH and then neutralized with 250 μL of glacial acetic acid. A 300-μL aliquot was then added to 5 mL of liquid scintillation fluid (Biosafe II; Research Products International) for counting, and a 30-μL aliquot was used for protein assay (Bradford; Bio-Rad). A 5-μL aliquot of the uptake solution was also counted as standard. Uptakes are expressed in pmol of K^+/mg of protein/min, and the furosemide-sensitive uptake (KCC-mediated flux) is calculated as the difference between the uptake measured in absence of furosemide and the flux obtained in the presence of 2 mM furosemide. Each experimental condition is measured in triplicate.

ACKNOWLEDGMENTS. We acknowledge the technical expertise of Lisa Diehl in generating the KCC2 overexpressing cell line. This work was funded by National Institutes of Health Grants R21 NS53658 (to E. Delpire), U54 MH074427 to C.D.W., and U54 MH084659 (to C.W.L.) and the Vanderbilt Specialized Chemistry Center for Accelerated Probe Development).

1. Woo N-S, et al. (2002) Hyper-excitability and epilepsy associated with disruption of the mouse neuronal-specific K-Cl cotransporter gene. *Hippocampus* 12:258–268.

2. Zhu L, Polley N, Mathews GC, Delpire E (2008) NKCC1 and KCC2 prevent hyperexcitability in the mouse hippocampus. *Epilepsy Res* 79:201–212.

3. Morgado C, Pinto-Ribeiro F, Tavares I (2008) Diabetes affects the expression of GABA and potassium chloride cotransporter in the spinal cord: A study in streptozotocin diabetic rats. *Neurosci Lett* 438:102–106.
4. Coull JA, et al. (2003) Trans-synaptic shift in anion gradient in spinal lamina I neurons as a mechanism of neuropathic pain. *Nature* 424:938–942.
5. Nomura H, Sakai A, Nagano M, Umino M, Suzuki H (2006) Expression changes of cation chloride cotransporters in the rat spinal cord following intraplantar formalin. *Neurosci Res* 56:435–440.
6. Jolivalt CG, Lee CA, Ramos KM, Calcutt NA (2008) Allodynia and hyperalgesia in diabetic rats are mediated by GABA and depletion of spinal potassium-chloride co-transporters. *Pain* 140:48–57.
7. Zhang W, Liu L-Y, Xu T-L (2008) Reduced potassium-chloride co-transporter expression in spinal cord dorsal horn neurons contributes to inflammatory pain hypersensitivity in rats. *Neuroscience* 10.1016/j.neuroscience. 2007.12.037.
8. Miletic G, Miletic V (2008) Loose ligation of the sciatic nerve is associated with TrkB receptor-dependent decreases in KCC2 protein levels in the ipsilateral spinal dorsal horn. *Pain* 137:532–539.
9. Cramer SW, et al. (2008) The role of cation-dependent chloride transporters in neuropathic pain following spinal cord injury. *Mol Pain* 4:36.
10. Rybak LP (1993) Ototoxicity of loop diuretics. *Otolaryngol Clin North Am* 26:829–844.
11. Ikeda K, Oshima T, Hidaka H, Takasaka T (1997) Molecular and clinical implications of loop diuretic ototoxicity. *Hearing Res* 107:1–8.
12. Delpire E, Lu J, England R, Dull C, Thorne T (1999) Deafness and imbalance associated with inactivation of the secretory Na-K-2Cl co-transporter. *Nat Genet* 22:192–195.
13. Lauf PK (1984) Thiol-dependent passive K/Cl transport in sheep red cells. IV. Furosemide inhibition as a function of external Rb^+, Na^+, and Cl^-. *J Membr Biol* 77:57–62.
14. Payne JA (1997) Functional characterization of the neuronal-specific K-Cl cotransporter: Implications for $[K^+]_o$ regulation. *Am J Physiol* 273:C1516–C1525.
15. Mercado A, Song L, Vazquez N, Mount DB, Gamba G (2000) Functional comparison of the K^+-Cl^- cotransporters KCC1 and KCC4. *J Biol Chem* 275:30326–30334.
16. Delpire E, Lauf PK (1992) Kinetics of DIDS inhibition of swelling-activated K-Cl cotransport in low K sheep erythrocytes. *J Membr Biol* 126:89–96.
17. Brugnara C, Kopin AS, Bunn HF, Tosteson DC (1985) Regulation of cation content and cell volume in erythrocytes from patients with homozygous hemoglobin C disease. *J Clin Invest* 75:1608–1617.
18. Jennings ML (1989) Structure and function of the red cell anion transport protein. *Annu Rev Biophys Biophys Chem* 18:397–430.
19. Kidd JF, Thorn P (2000) Intracellular Ca^{2+} and Cl^- channel activation in secretory cells. *Annu Rev Physiol* 62:493–513.
20. Weaver CD, Harden D, Dworetzky SI, Robertson B, Knox RJ (2004) A thallium-sensitive, fluorescence-based assay for detecting and characterizing potassium channel modulators in mammalian cells. *J Biomol Screen* 9:671–677.
21. Muanprasat C, et al. (2004) Discovery of glycine hydrazide pore-occluding CFTR inhibitors: Mechanism, structure–activity analysis, and in vivo efficacy. *J Gen Physiol* 124:125–137.
22. De La Fuente R, Namkung W, Mills A, Verkman AS (2008) Small-molecule screen identifies inhibitors of a human intestinal calcium-activated chloride channel. *Mol Pharmacol* 73:758–768.
23. Payne JA, Stevenson TJ, Donaldson LF (1996) Molecular characterization of a putative K-Cl cotransporter in rat brain. A neuronal-specific isoform. *J Biol Chem* 271:16245–16252.
24. DeFazio RA, Keros S, Quick MW, Hablitz JJ (2000) Potassium-coupled chloride cotransport controls intracellular chloride in rat neocortical pyramidal neurons. *J Neurosci* 20:8069–8076.
25. Pathak HR, et al. (2007) Disrupted dentate granule cell chloride regulation enhances synaptic excitability during development of temporal lobe epilepsy. *J Neurosci* 27:14012–14022.
26. Banke TG, Gegelashvili G (2008) Tonic activation of group I mGluRs modulates inhibitory synaptic strength by regulating KCC2 activity. *J Physiol* 586:4925–4934.
27. Hubner CA, et al. (2001) Disruption of KCC2 reveals an essential role of K-Cl cotransport already in early synaptic inhibition. *Neuron* 30:515–524.
28. Zhu L, Lovinger D, Delpire E (2005) Cortical neurons lacking KCC2 expression show impaired regulation of intracellular chloride. *J Neurophysiol* 93:1557–1568.
29. Hekmat-Scafe DS, Lundy MY, Ranga R, Tanouye MA (2006) Mutations in the K^+/Cl^- cotransporter gene kazachoc (kcc) increase seizure susceptibility in *Drosophila*. *J Neurosci* 26:8943–8954.
30. Reynolds A, et al. (2008) Neurogenic role of the depolarizing chloride gradient revealed by global overexpression of KCC2 from the onset of development. *J Neurosci* 28:1588–1597.
31. Ingram TT (1964) Today's drugs. Frusemide. *Br Med J* 2:1640–1641.
32. Asbury MJ, Gatenby PB, O'Sullivan S, Bourke E (1972) Bumetanide: Potent new ''loop'' diuretic. *Br Med J* 1:211–213.
33. Dunham PB, Steward GW, Ellory JC (1980) Chloride-activated passive potassium transport in human erythrocytes. *Proc Natl Acad Sci USA* 77:1711–1715.
34. Lauf PK, Theg BE (1980) A chloride dependent K^+ flux induced by *N*-ethylmaleimide in genetically low K^+ sheep and goat erythrocytes. *Biochem Biophys Res Commun* 70:221–242.
35. Garay RP, Nazaret C, Hannaert PA, Cragoe EJ, Jr (1988) Demonstration of a $[K^+Cl^-]$-cotransport system in human red cells by its sensitivity to [(dihydroindenyl)oxy]alkanoic acids: Regulation of cell swelling and distinction from the bumetanide-sensitive $[Na^+, K^+, Cl^-]$-cotransport system. *Mol Pharmacol* 33:696–701.
36. Delpire E (2000) Cation-chloride cotransporters in neuronal communication. *News Physiol Sci* 15:309–312.
37. Kahle KT, et al. (2008) Roles of the cation–chloride cotransporters in neurological disease. *Nat Clin Pract Neurol* 4:490–503.
38. Segel IH (1975) *Enzyme Kinetics. Behavior and Analysis of Rapid Equilibrium and Steady-State Enzyme Systems* (Wiley, New York).
39. Delpire E, Lauf PK (1991) Kinetics of Cl-dependent K fluxes in hyposmotically low K sheep erythrocytes. *J Gen Physiol* 97:173–193.
40. Delpire E, Lauf PK (1991) Trans-effects of cellular K and Cl on ouabain-resistant Rb(K) influx in low K sheep red blood cells: Further evidence for asymmetry of K-Cl cotransport. *Pflügers Arch* 419:540–542.
41. Cha S (1968) A simple method for derivation of rate equations for enzyme-catalyzed reactions under the rapid equilibrium assumption or combined assumptions of equilibrium and steady state. *J Biol Chem* 243:820–825.